Supplementary Material (ESI) for New Journal of Chemistry

Boronic acid based photoinduced electron transfer (PET) fluorescence sensors for saccharides

Joseph D. Larkin, Karine A. Frimat, Thomas M. Fyles, Stephen E. Flower and Tony D. James

2-*o*-Tolyl-[1,3,2] dioxaborinane

To a stirred solution of *o*-tolylboronic acid (2.50 g, 18.40 mmol) in toluene (70 cm^3) was added 1,3-propanediol (2.80 g, 36.80 mmol). The mixture was heated and stirred under Dean and Stark conditions for 1 hour. After cooling, the reaction mixture was washed with water (50 cm^3) and dried ($MgSO_4$). The solvent was removed under reduced pressure affording 2-*o*-tolyl-[1,3,2] dioxaborinane as a dark yellow oil (2.97 g, 91.7 %). δ_H(400 MHz; $CDCl_3$) 2.04-2.05 (2H, m), 2.55 (3H, s), 4.19 (4H, t, *J* 5.4 Hz), 7.16-7.20 (2H, m), 7.29-7.31 (1H, m), 7.32-7.77 (1H, m); δ_C(100MHz; $CDCl_3$) 22.5, 27.5, 61.9, 124.5, 129.8, 134.6, 143.7; *m/z* (EI^+) 176 (100 %, M^+).

2-(2-Bromomethyl-phenyl)-[1,3,2] dioxaborinane (13)

To a stirred solution of 2-*o*-tolyl-[1,3,2] dioxaborinane (2.94 g, 16.70 mmol) in benzene (60 cm^3) was added *N*-bromosuccinimide (3.10 g, 17.60 mmol) and AIBN (0.30 g). The mixture was heated and stirred under reflux for 2 hours. The resulting mixture was then cooled on an ice-water-bath and the precipitate was removed by filtration. The filtrate solvent was removed under reduced pressure and the crude product was purified by silica gel chromatography eluting with n-hexane:chloroform (1:5) to afford the dioxaborinane **13** as a yellow oil (2.55 g, 60.1 %), (Found: C, 47.1; H, 4.6. Calc. For $C_{10}H_{12}BBrO_2$: C, 47.1; H, 4.7 %). δ_H(400 MHz; $CDCl_3$) 2.06-2.52 (2H, m), 4.19 (4H, t, *J* 5.4 Hz), 4.92 (2H, s), 7.25-7.92 (4H, m); δ_C(100 MHz; $CDCl_3$) 27.3, 27.5, 62.1, 127.4, 130.0, 130.2, 135.2, 143.2; *m/z* (EI^+) 253 (1.8 %, $[M - H]^+$ and 175 (96, $[M - Br]^+$).

9,10-Bis[(methylamino)methyl]anthracene (27)

Methylamine (7.5 cm^3 of a 2.0 $moldm^{-3}$ solution in methanol, 15.00 mmol) was added under argon atmosphere to a solution of 9,10-dialdehyde anthracene **25** (1.17 g, 5.00 mmol) in methanol (20 cm^3) a stirred round-bottomed flask at room temperature. After stirring overnight, a solution of sodium borohydride (0.93 g, 25.00 mmol) in dry methanol (10 cm^3) was added in one portion and the reaction mixture was stirred for 4 hours before being poured onto 50 cm^3 of water. The aqueous layer was extracted with dichloromethane (3 x 50 cm^3). The combined organic extracts were dried ($MgSO_4$), filtered, and concentrated under reduced pressure to give the diamine **27** as a yellow-orange powder (1.10 g, 83.2 %), mp 139-140°C. δ_H(300 MHz, $CDCl_3$) 2.58 (6H, s), 4.70 (4H, s),

7.59 (4H, dd, J 6.9 Hz, J 3.3 Hz), 8.41 (4H, dd, J 6.9 Hz, J 3.3 Hz,); δ_C(75 MHz, $CDCl_3$) 37.2, 48.0, 124.9, 125.72, 130.2, 132.0; *m/z* (FAB^+) 265 (32 %, $[M + H]^+$) and 234 (100, $[M - CH_3NH]^+$).

9,10-Bis[[*N*-methyl-*N*-(o-boronobenzyl)amino]methyl]anthracene (1)

To a stirred solution of diamine **27** (0.53 g, 2.00 mmol) in 50 cm^3 of dry acetonitrile was added the benzyl bromide **13** (1.52 g, 6.00 mmol), followed by K_2CO_3 (1.10 g, 8.00 mmol). The reaction mixture was then allowed to stir under reflux overnight. The acetonitrile was removed under reduced pressure and water (50 cm^3) was added. The aqueous layer was then extracted with dichloromethane (3 x 50 cm^3) and the organic layers were combined, dried ($MgSO_4$) and then concentrated under reduced pressure to afford crude **1**. The crude material was purified by trituration with ethyl acetate to give **1** as a yellow orange powder (0.30 g, 28.2 %), mp 188-190°C (decomp.). δ_H(300 MHz; $CDCl_3$/ CD_3OD 1:1) 2.19 (6H, s), 3.90 (4H, s), 4.46 (4H, s,), 7.28-8.38 (16H, m); *m/z* (FAB^+) 645 (24 %, $[M - 4 \times H_2O + 2 \times \text{glycerol} + H]^+$) and 205 (100, $[CH_2AnthCH_2 + H]^+$).

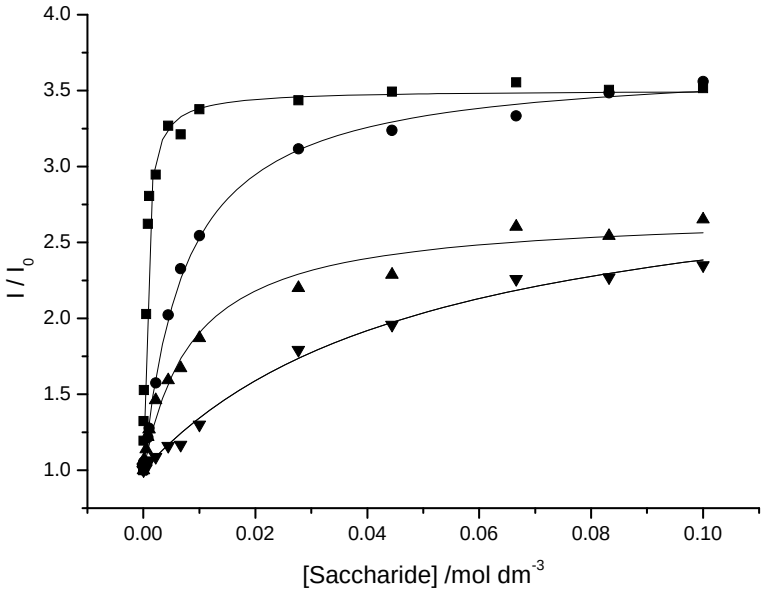

Figure 1S. Relative fluorescence intensity vs. Saccharide concentration profile of sensor **1** (1×10^{-7} moldm^{-3}) (■) D- glucose, (●) D-fructose, (▲) D-galactose; (▼) D-mannose in 52.1 wt% MeOH pH 8.21 phosphate buffer at 25 °C; λ_{ex} = 370 nm, λ_{em} = 422 nm.

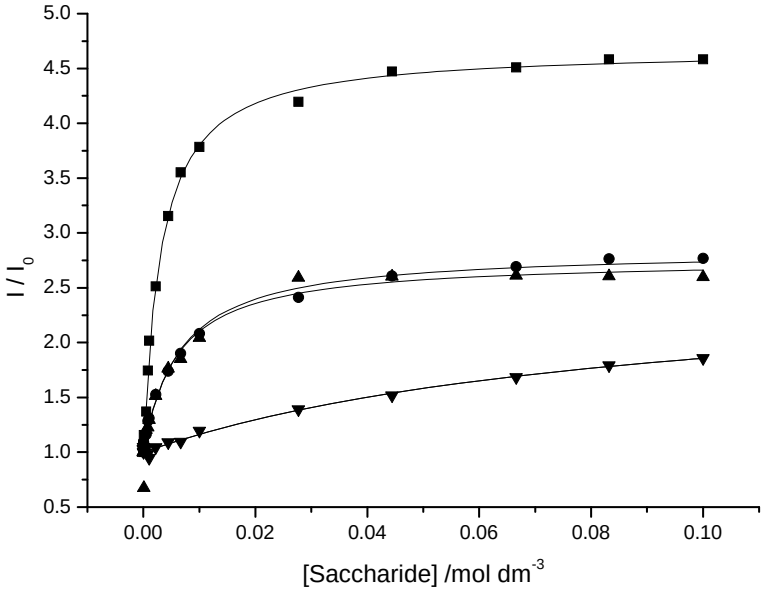

Figure 2S. Relative fluorescence intensity vs. Saccharide concentration profile of sensor **3** (1×10^{-7} moldm^{-3}) (■) D- glucose, (●) D-fructose, (▲) D-galactose; (▼) D-mannose in 52.1 wt% MeOH pH 8.21 phosphate buffer at 25 °C; λ_{ex} = 271 nm, λ_{em} = 339 nm.

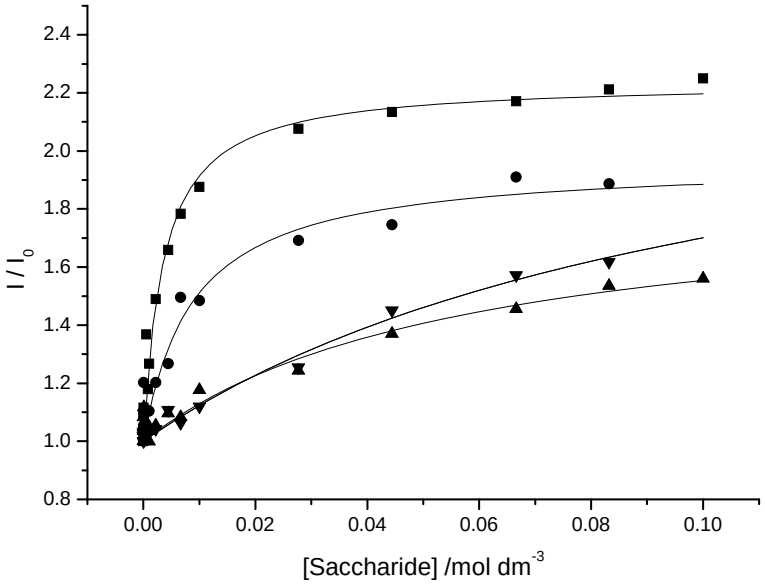

Figure 3S. Relative fluorescence intensity vs. Saccharide concentration profile of sensor **4** (1×10^{-7} moldm^{-3}) (■) D- glucose, (●) D-fructose, (▲) D-galactose; (▼) D-mannose in 52.1 wt% MeOH pH 8.21 phosphate buffer at 25 °C; λ_{ex} = 370 nm, λ_{em} = 416 nm.

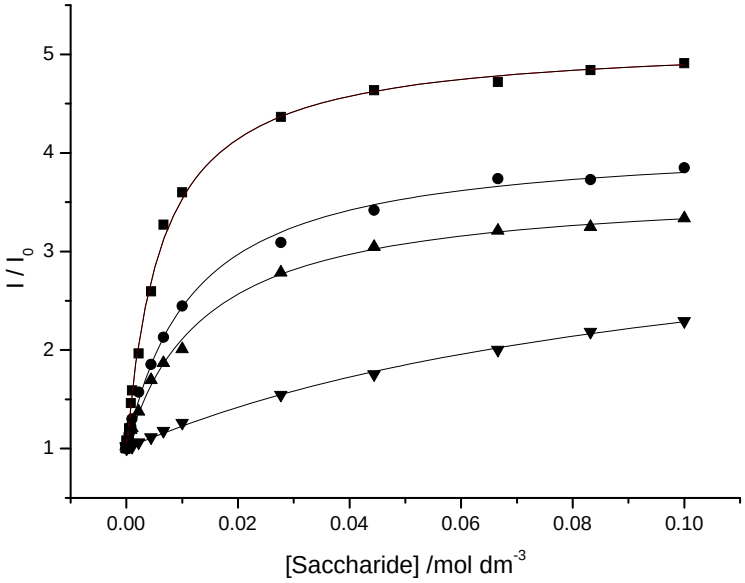

Figure 4S. Relative fluorescence intensity vs. Saccharide concentration profile of sensor **5**(1×10^{-7} moldm^{-3}) (■) D- glucose, (●) D-fructose, (▲) D-galactose; (▼) D-mannose in 52.1 wt% MeOH pH 8.21 phosphate buffer at 25 °C; λ_{ex} = 343 nm, λ_{em} = 397 nm.

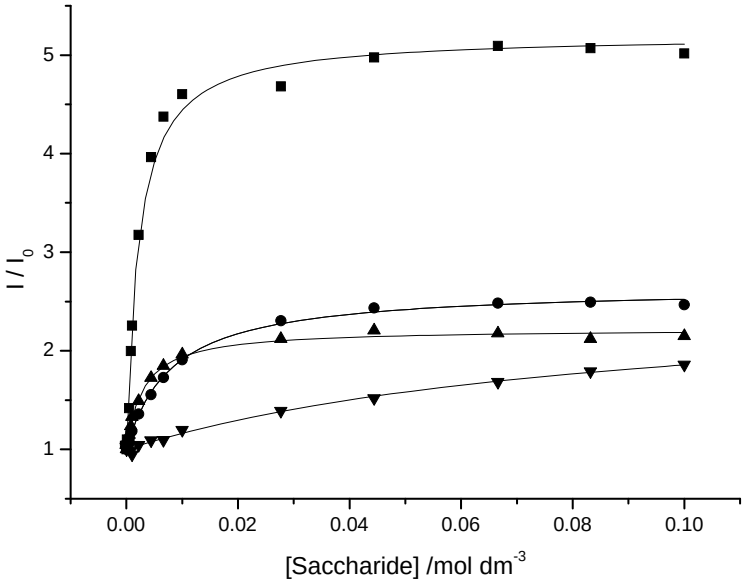

Figure 5S. Relative fluorescence intensity vs. Saccharide concentration profile of sensor **6** (1×10^{-7} moldm^{-3}) (■) D- glucose, (●) D-fructose, (▲) D-galactose; (▼) D-mannose in 52.1 wt% MeOH pH 8.21 phosphate buffer at 25 °C; λ_{ex} = 271 nm, λ_{em} = 343 nm.

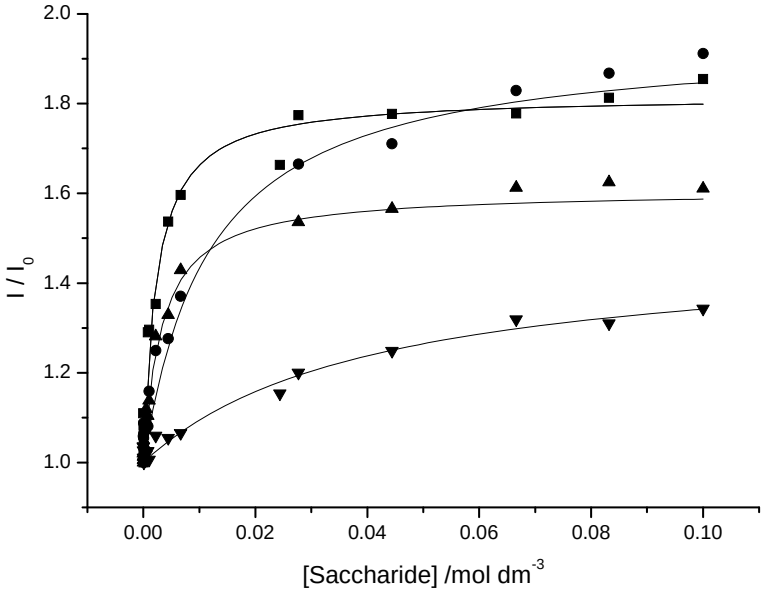

Figure 6S. Relative fluorescence intensity vs. Saccharide concentration profile of sensor **7** (1×10^{-7} moldm^{-3}) (■) D- glucose, (●) D-fructose, (▲) D-galactose; (▼) D-mannose in 52.1 wt% MeOH pH 8.21 phosphate buffer at 25 °C; λ_{ex} = 370 nm, λ_{em} = 417 nm.

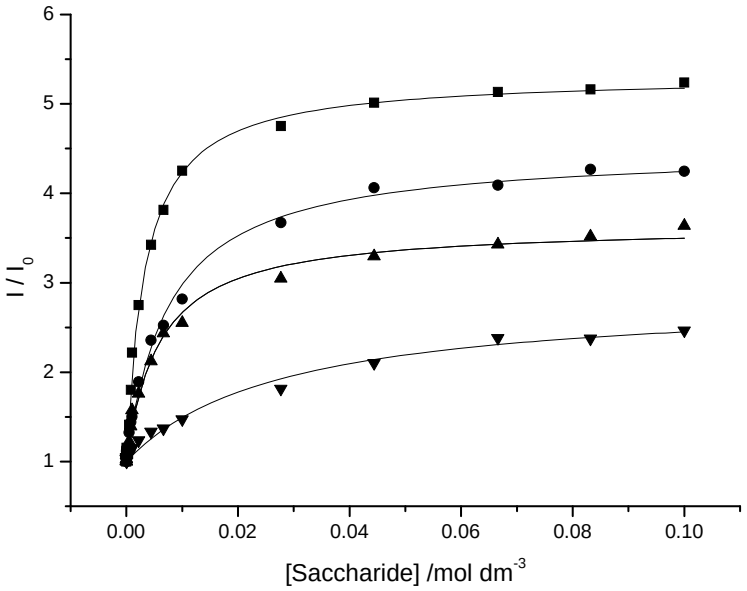

Figure 7S. Relative fluorescence intensity vs. Saccharide concentration profile of sensor **8** (1×10^{-7} moldm^{-3}) (■) D- glucose, (●) D-fructose, (▲) D-galactose; (▼) D-mannose in 52.1 wt% MeOH pH 8.21 phosphate buffer at 25 °C; λ_{ex} = 343 nm, λ_{em} = 397 nm.

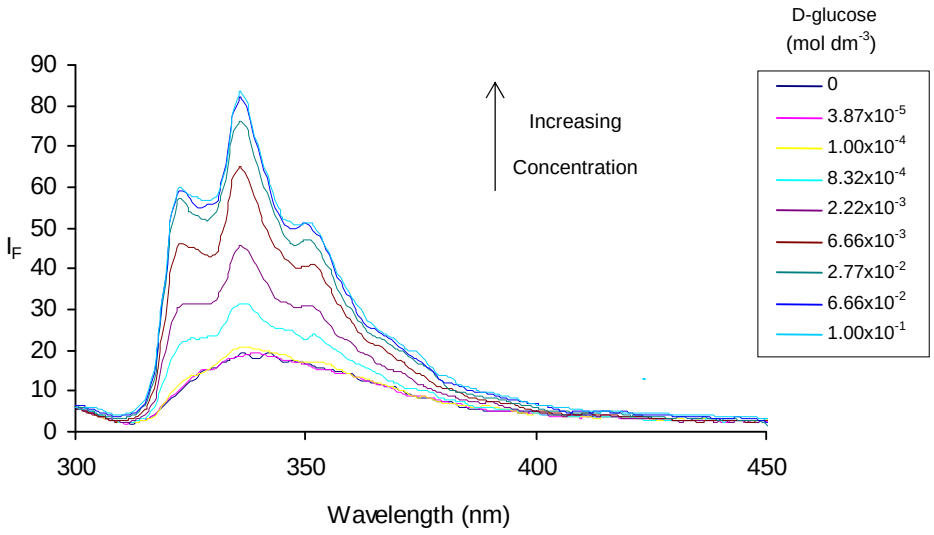

Figure 8S. Fluorescence Intensity (I_F) of Sensor **3** with increasing concentration of D-glucose at pH 8.21.

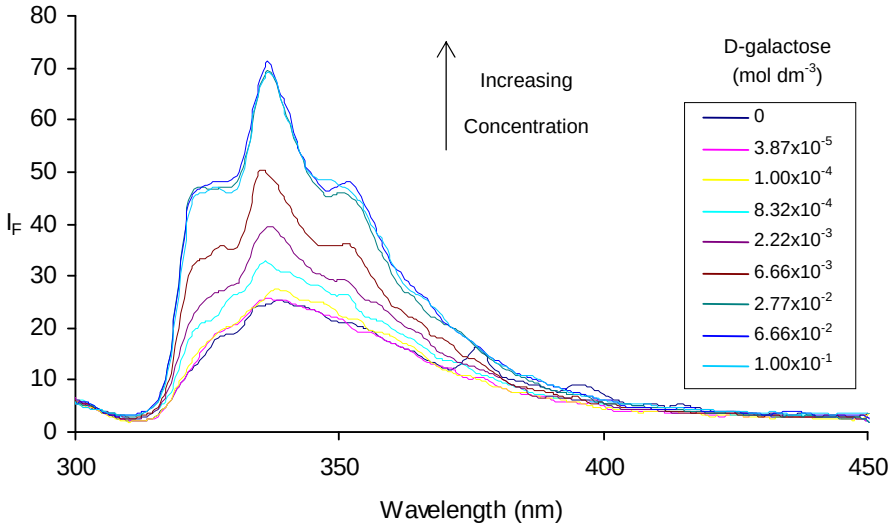

Figure 9S. Fluorescence Intensity (I_F) of Sensor **3** with increasing concentration of D-galactose at pH 8.21.

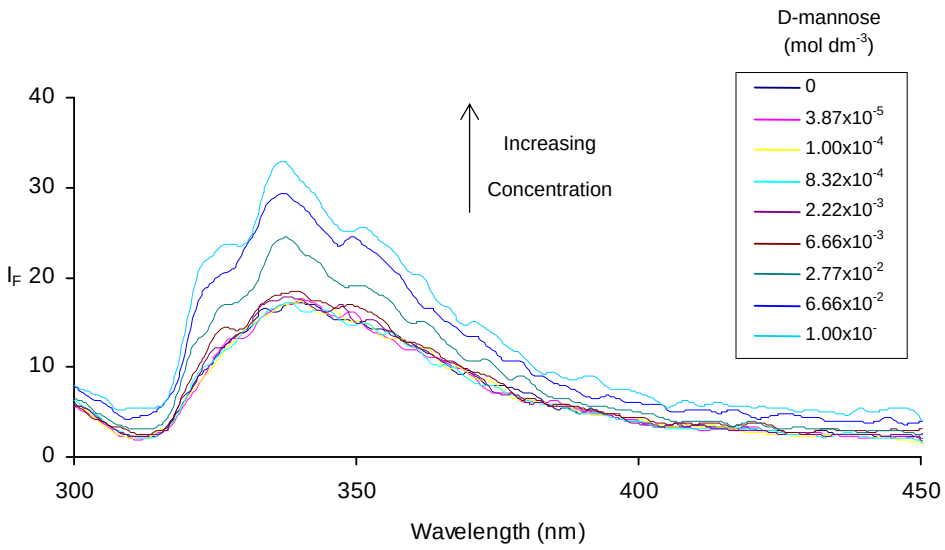

Figure 10S. Fluorescence Intensity (I_F) of Sensor **3** with increasing concentration of D-mannose at pH 8.21.

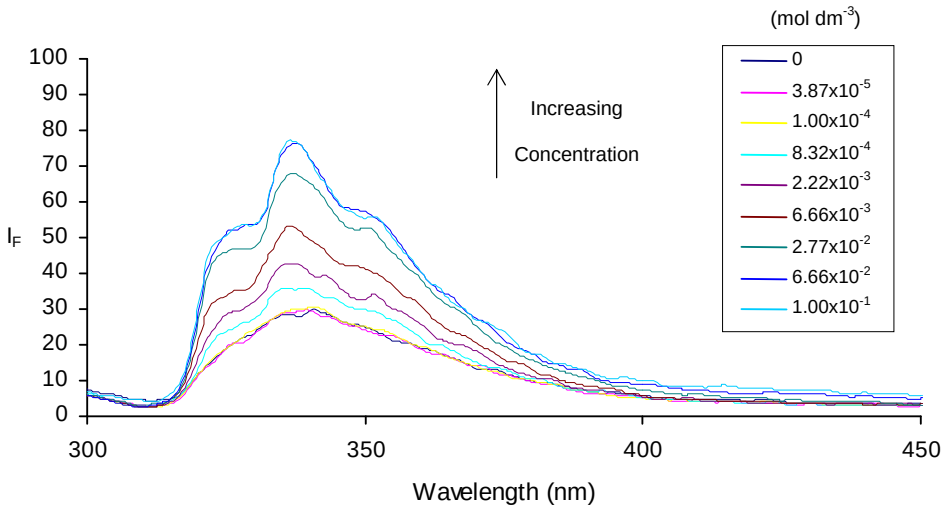

Figure 11S. Fluorescence Intensity (I_F) of Sensor **3** with increasing concentration of D-fructose at pH 8.21.

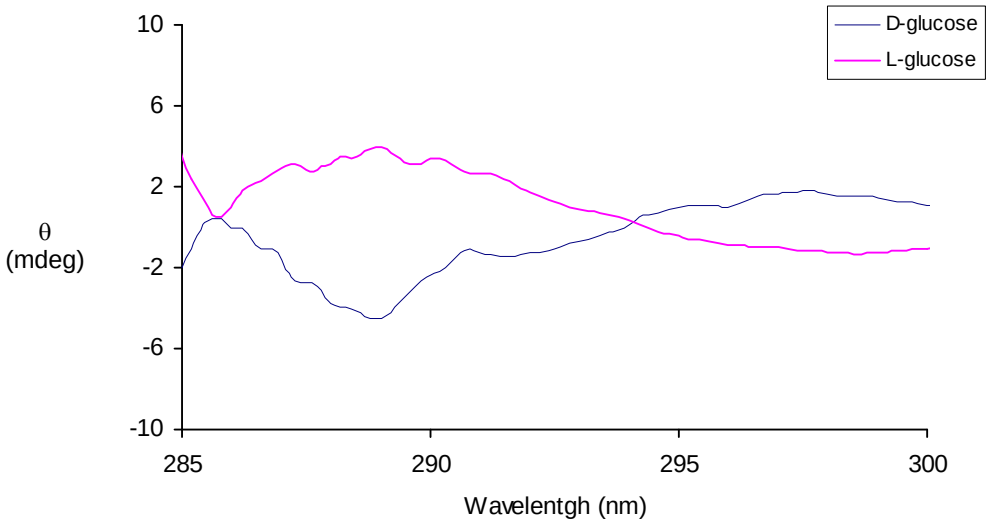

Figure 12S. CD Spectra of Sensor **3** in the presence of D-or L-glucose.

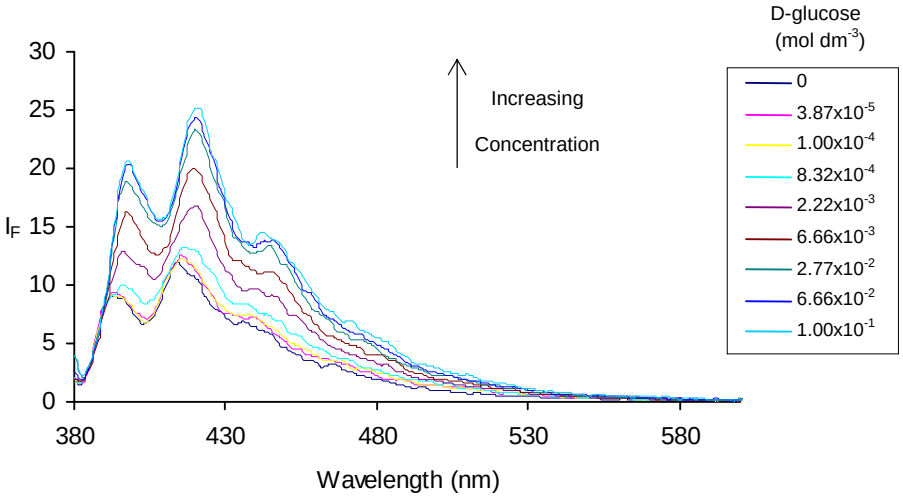

Figure 13S. Fluorescence Intensity (I_F) of Sensor **4** with increasing concentration of D-glucose at pH 8.21.

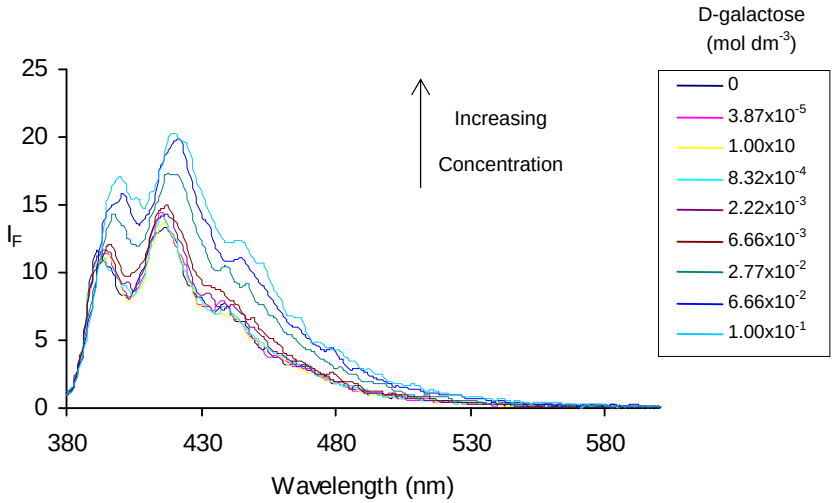

Figure 14S. Fluorescence Intensity (I_F) of Sensor **4** with increasing concentration of D-galactose at pH 8.21.

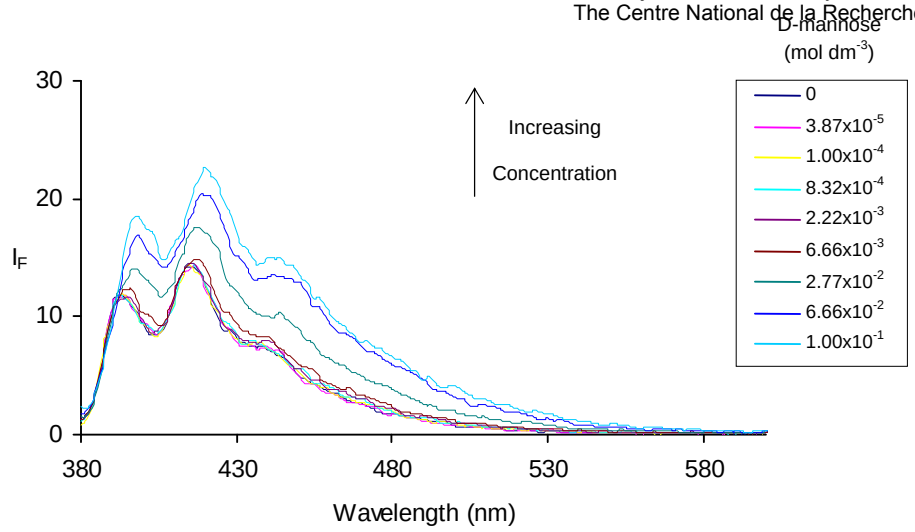

Figure 15S. Fluorescence Intensity (I_F) of Sensor **4** with increasing concentration of D-mannose at pH 8.21.

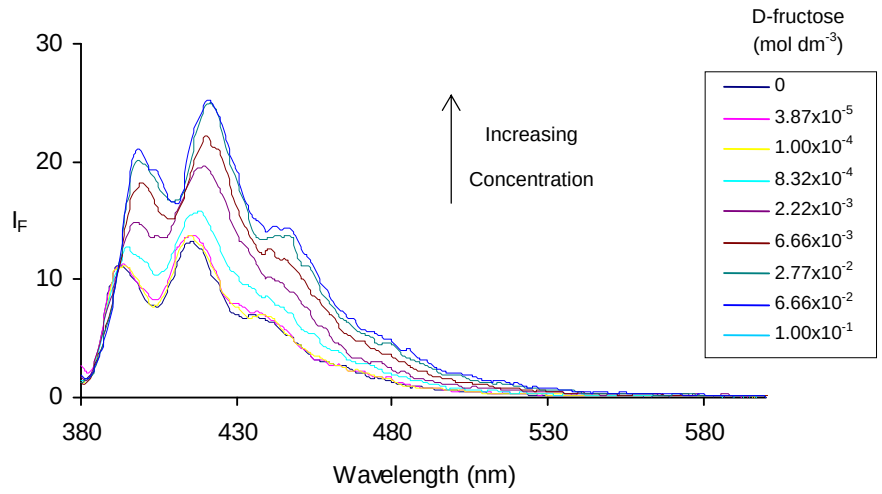

Figure 16S. Fluorescence Intensity (I_F) of Sensor **4** with increasing concentration of D-fructose at pH 8.21.

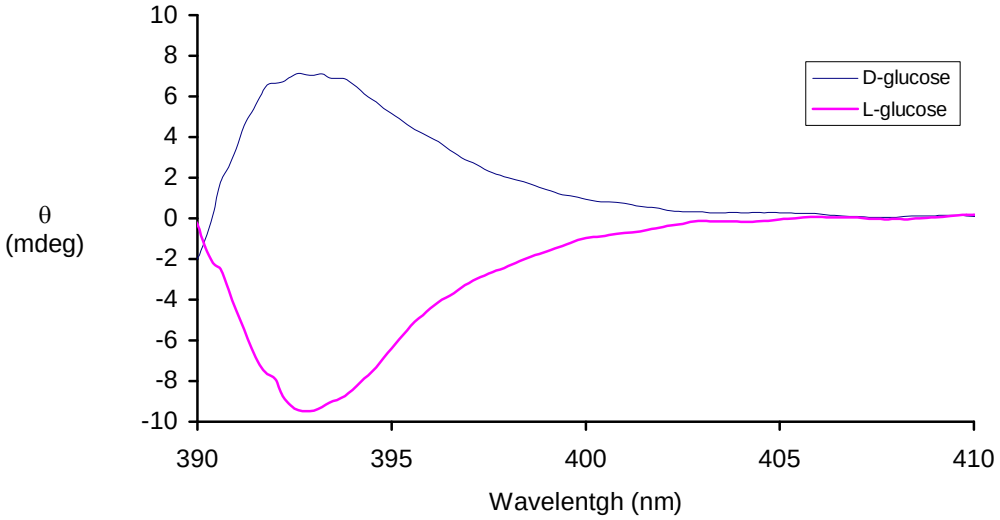

Figure 17S. CD Spectra of Sensor **4** in the presence of D-or L-glucose.

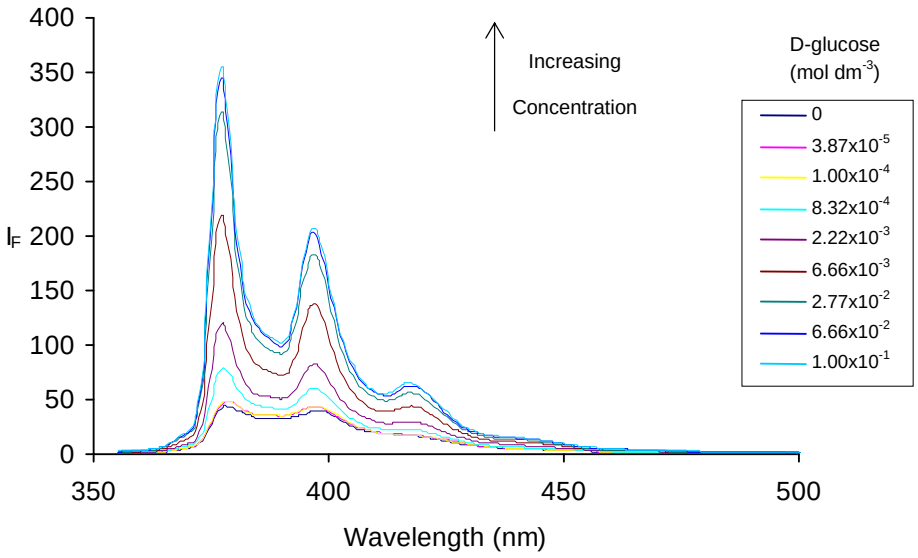

Figure 18S. Fluorescence Intensity (I_F) of Sensor **5** with increasing concentration of D-glucose at pH 8.21.

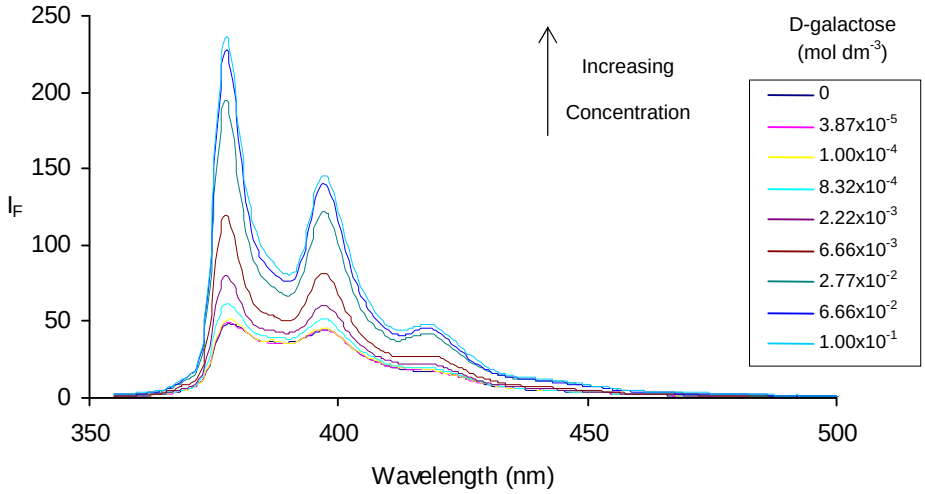

Figure 19S. Fluorescence Intensity (I_F) of Sensor **5** with increasing concentration of D-galactose at pH 8.21.

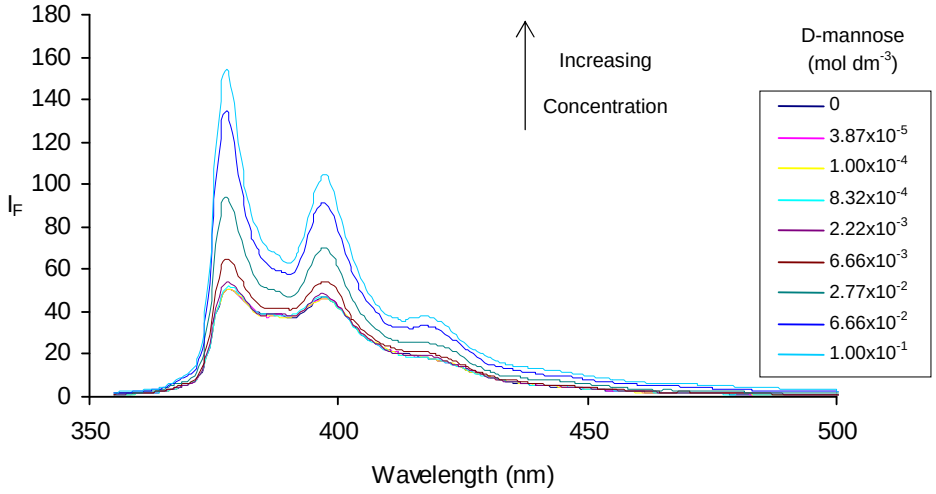

Figure 20S. Fluorescence Intensity (I_F) of Sensor **5** with increasing concentration of D-mannose at pH 8.21.

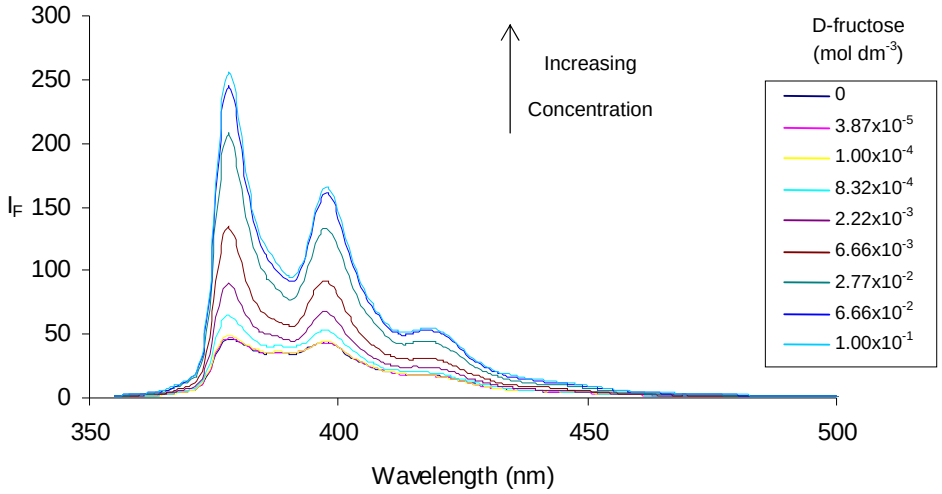

Figure 21S. Fluorescence Intensity (I_F) of Sensor **5** with increasing concentration of D-fructose at pH 8.21.

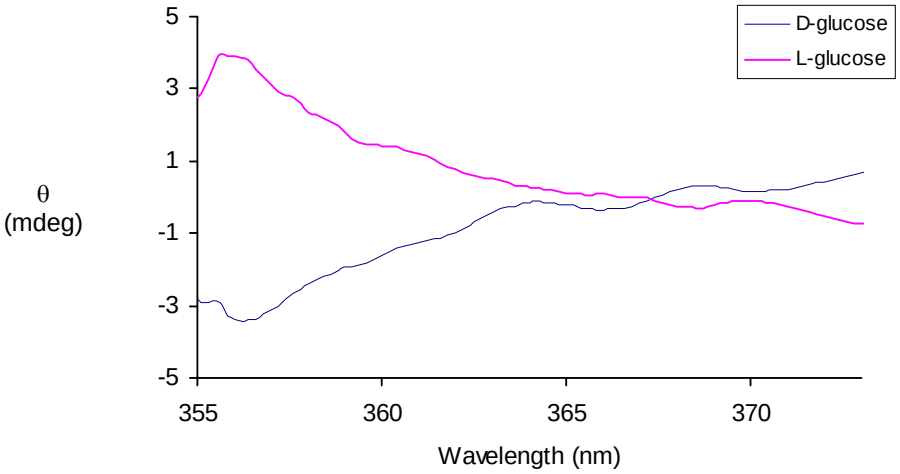

Figure 22S. CD Spectra of Sensor **5** in the presence of D-or L-glucose.

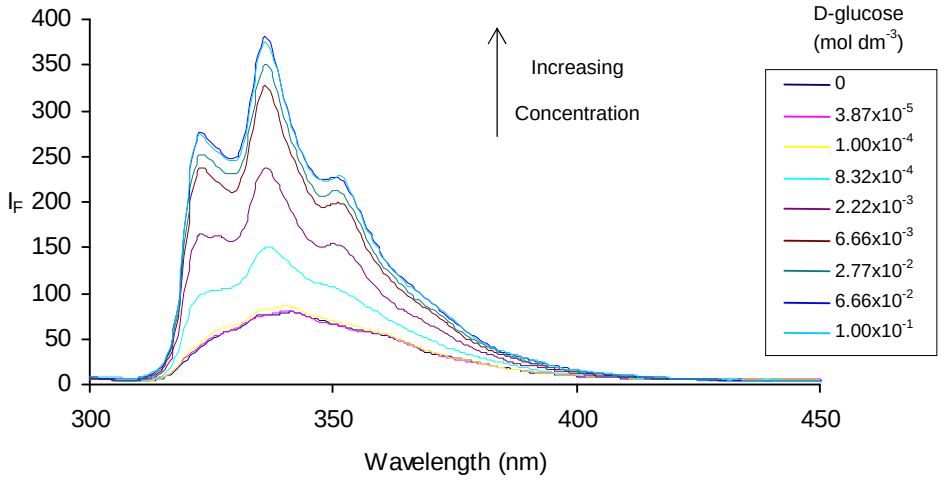

Figure 23S. Fluorescence Intensity (I_F) of Sensor **6** with increasing concentration of D-glucose at pH 8.21.

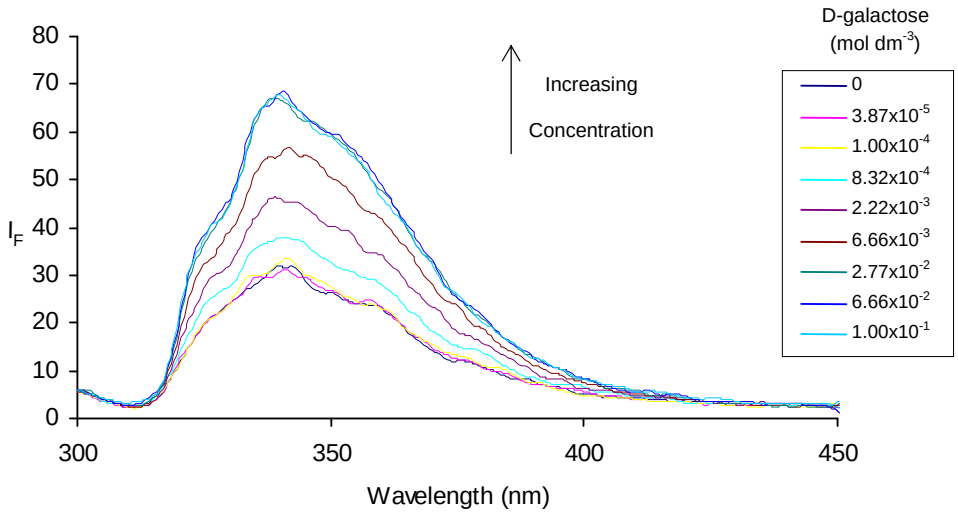

Figure 24S. Fluorescence Intensity (I_F) of Sensor **6** with increasing concentration of D-galactose at pH 8.21.

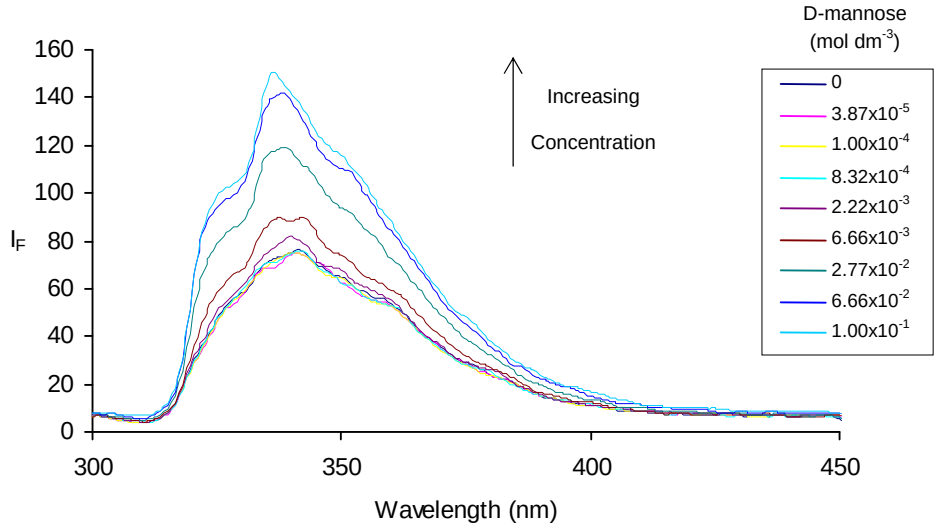

Figure 25S. Fluorescence Intensity (I_F) of Sensor **6** with increasing concentration of D-mannose at pH 8.21.

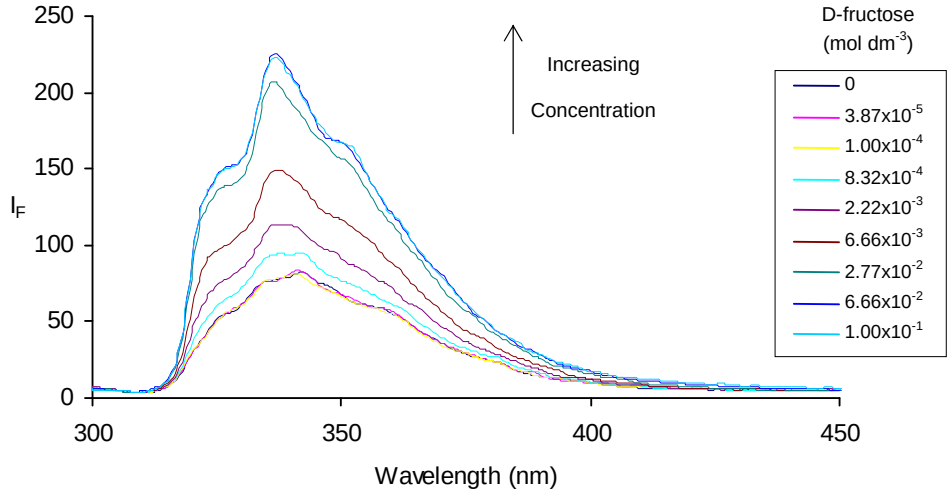

Figure 26S. Fluorescence Intensity (I_F) of Sensor **6** with increasing concentration of D-fructose at pH 8.21.

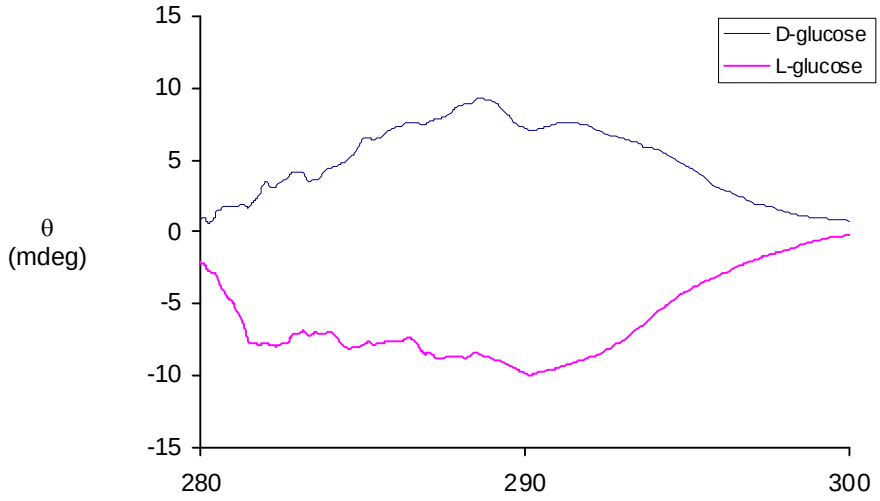

Figure 27S. CD Spectra of Sensor **6** in the presence of D-or L-glucose.

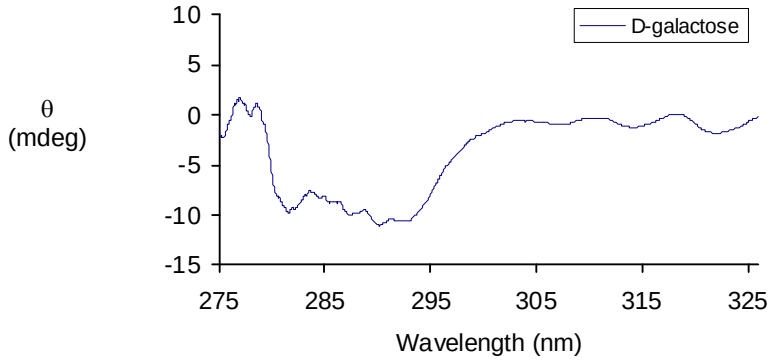

Figure 28S. CD Spectra of Sensor **6** in the presence of D-galactose.

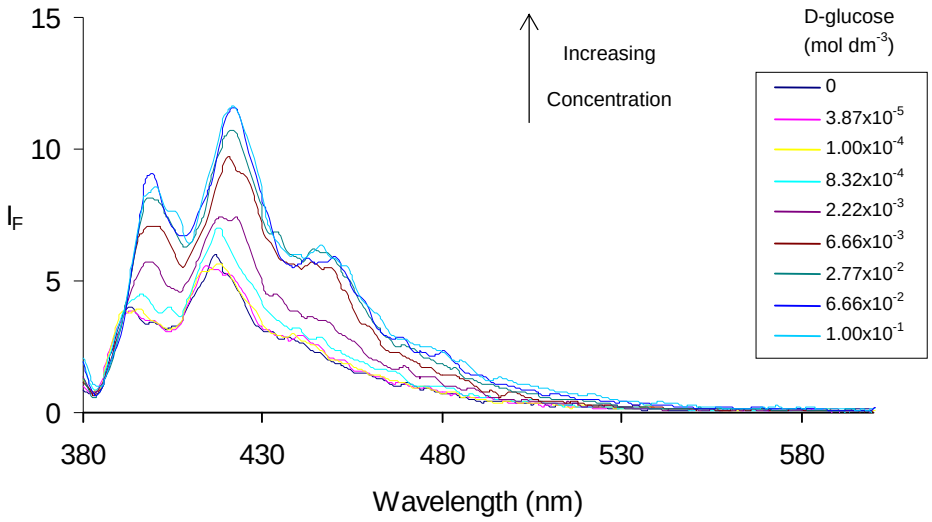

Figure 29S. Fluorescence Intensity (I_F) of Sensor **7** with increasing concentration of D-glucose at pH 8.21.

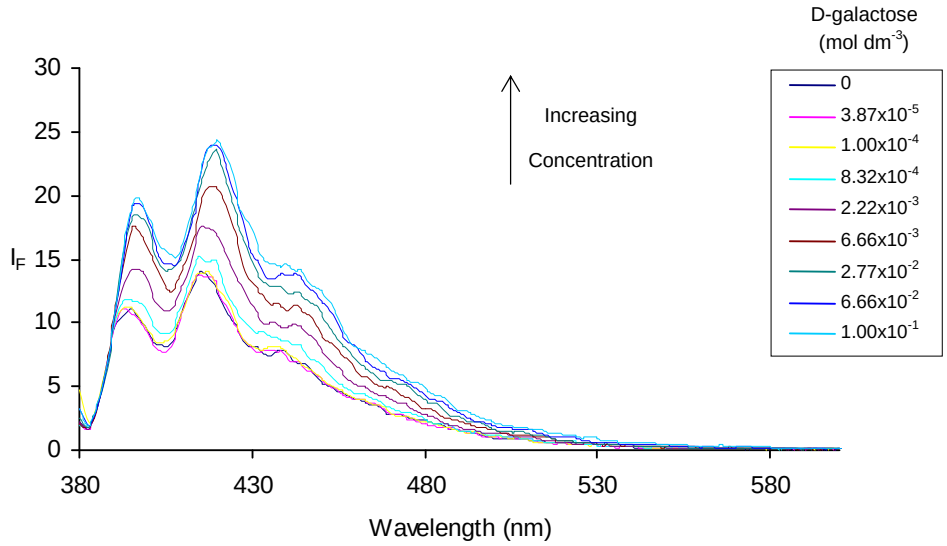

Figure 30S. Fluorescence Intensity (I_F) of Sensor **7** with increasing concentration of D-galactose at pH 8.21.

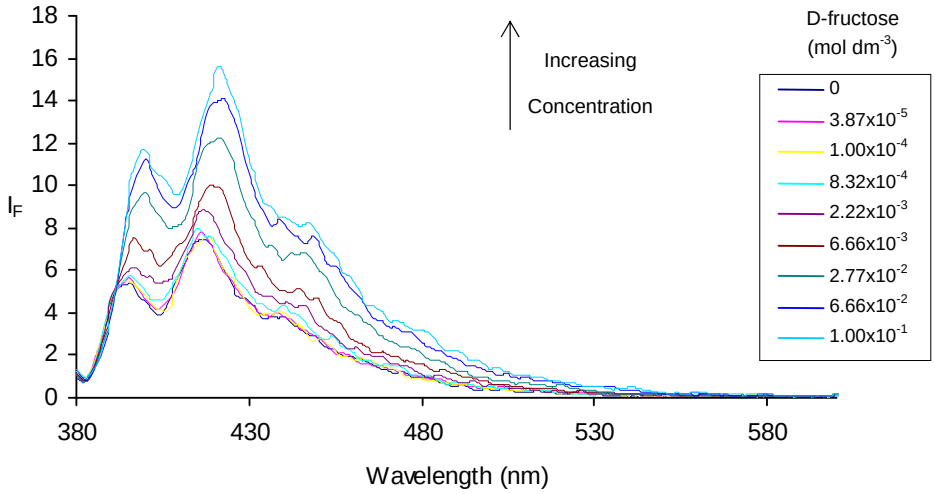

Figure 31S. Fluorescence Intensity (I_F) of Sensor **7** with increasing concentration of D-fructose at pH 8.21.

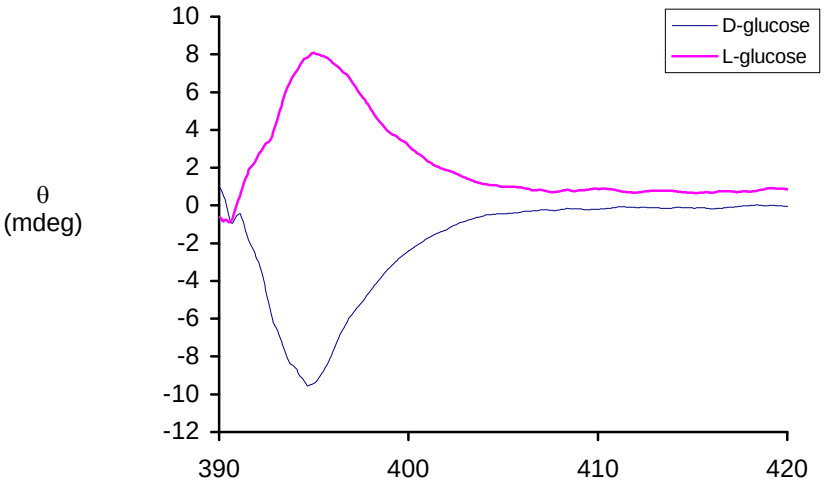

Figure 32S. CD Spectra of Sensor **7** in the presence of D-and L-glucose.

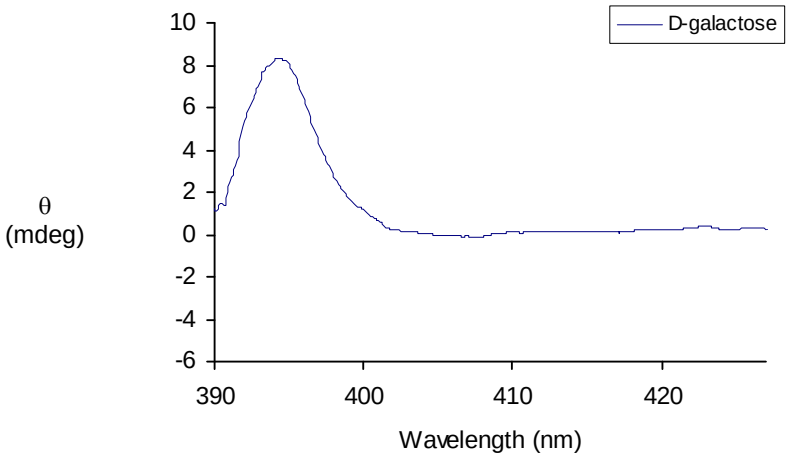

Figure 33S. CD Spectra of Sensor **7** in the presence of D-galactose.

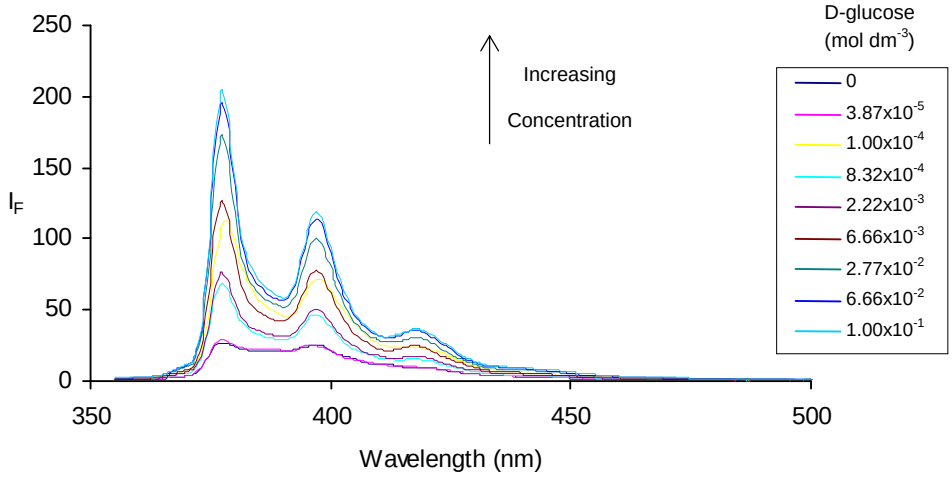

Figure 34S. Fluorescence Intensity (I_F) of Sensor **8** with increasing concentration of D-glucose at pH 8.21.

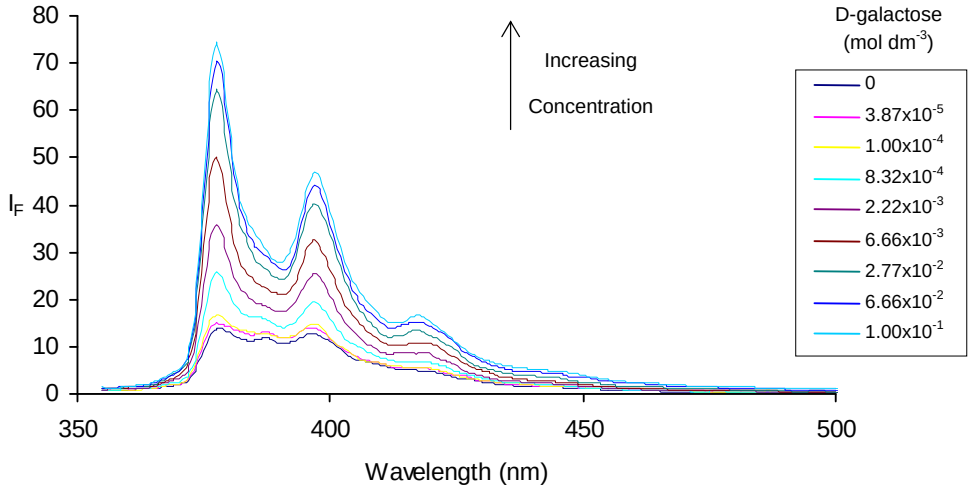

Figure 35S. Fluorescence Intensity (I_F) of Sensor **8** with increasing concentration of D-galactose at pH 8.21.

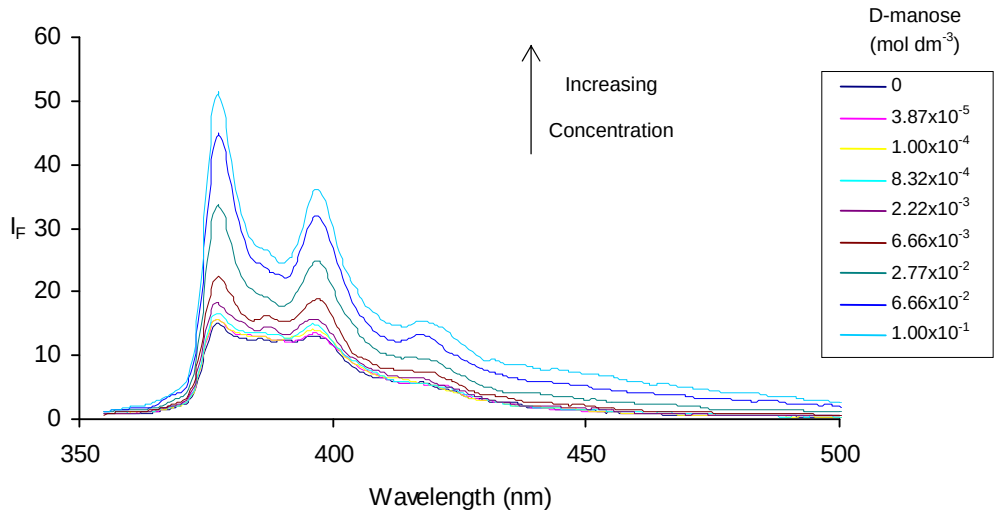

Figure 36S. Fluorescence Intensity (I_F) of Sensor **8** with increasing concentration of D-mannose at pH 8.21.

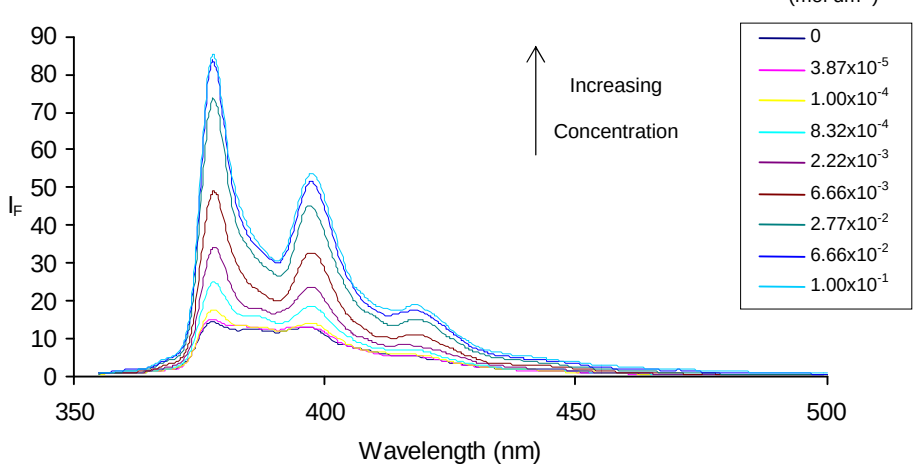

Figure 37S. Fluorescence Intensity (I_F) of Sensor **8** with increasing concentration of D-fructose at pH 8.21.

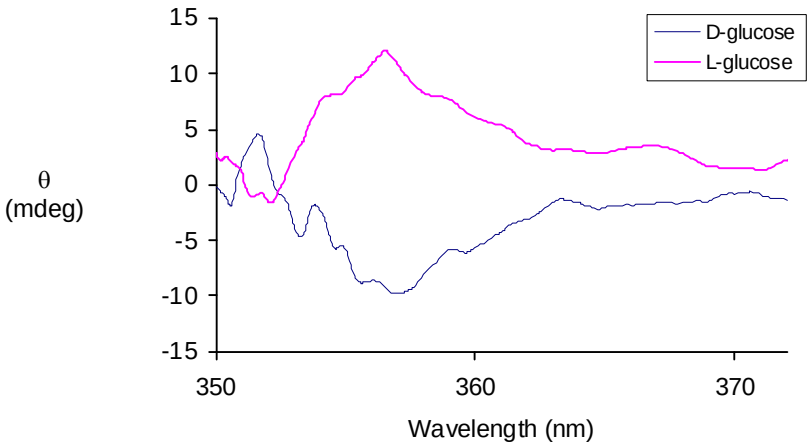

Figure 38S. CD Spectra of Sensor **8** in the presence of D-and L-glucose.